



## IoT and Cloud based Feature Extraction and Classification Model for Automatic Glaucoma Detection

R. Anandh<sup>1</sup> and G. Indirani<sup>2</sup>

<sup>1</sup>Research Scholar, Department of Computer Science and Engineering,  
FEAT, Annamalai University, Chidambaram (Tamilnadu), India.

<sup>2</sup>Associate Professor, Department of Computer Science and Engineering,  
Government College of Engineering, (Deputed from Annamalai University) Bargur (Tamilnadu), India.

(Corresponding author: R. Anandh)

(Received 13 November 2019, Revised 31 December 2019, Accepted 05 January 2020)

(Published by Research Trend, Website: [www.researchtrend.net](http://www.researchtrend.net))

**ABSTRACT:** Internet of Things (IoT) and cloud computing are interdependent domains that find useful for monitoring the patients located in remote areas by provisioning incessant support from physicians. For effective disease management, it is needed to design a model that makes use of IoT gadgets to predict the likelihood of the presence of a disease. In this paper, a new automated glaucoma recognition and classifier approach for the identification of the glaucoma diseases from the color fundus images. At first, the real color fundus images hold a collection of three RGB channels and the red channel gets extracted for further processes. Afterward, the contrast enhancement process gets executed by the use of an adaptive histogram equalization (AHE) model for improvising the contrast level of the image. Subsequently, a bilateral filtering technique is given to discard the noise that exists in the image. Afterward, a Directional local ternary quantized extrema pattern (DLTerQEP) based feature extraction process takes place. Then, the extracted features undergo classification by the use of a multi-class support vector machine (MSVM) model to classify the presence of glaucoma. The proposed model is tested using a DRISHTI-GS holds a sum of 101 retinal fundus images. The simulation outcome presented the advantage of the projected approach over the compared approaches.

**Keywords:** Classification, Cloud, Healthcare, IoT, Glaucoma.

**Abbreviations:** MSVM, Multi-Class Support Vector Machine; DLTerQEP, Directional local ternary quantized extrema pattern; AHE, Adaptive Histogram Equalization; IoT, Internet of Things; IoMT, Internet of Medical Things; OCT, Optical Coherence Tomography; FT, Fourier Transform; kNN, k-Nearest Neighbor (kNN) Classification; DTEC, Directional Ternary Extrema Coding.

### I. INTRODUCTION

Exponential develop the data with MEMS technology guided for the process Internet of Things (IoT) permits clients, objects, data and virtualized platforms in the surrounding interfaces by one another [1]. Different purposes create utilize of IoT in information collecting procedures from intelligence surrounding such transports, homes, hospitals, cities, etc. Due to developing the IoT dependent healthcare devices and sensors, some of the explores is illustrating the attention in the domain [2]. In the growing of pricey medicine with the occurrence of different diseases worldwide; it essentially needed the rebellion of healthcare from the hospital centered formation to a patient-centered model. For focusing on the method of controlling diseases, it is required for developing the system which creates utilization of everywhere sensing capabilities of IoT tools to forecasting the possibilities of important diseases in a patient.

IoT as well as cloud computing are interconnected and finds useful for observing the patients in the distant regions with contribution seamless maintenance from physicians with caretakers [3]. IoT is preserved with virtualized unrestrained capabilities with assets of the cloud for balancing the practical restrictions such as storage, power, and computation. Simultaneously, the

cloud suggests benefits from IoT with additional of the possibility of managing actual things in the real world by providing several services in a shared with dynamic manner. So, IoT with the cloud concept could be utilized for growing novel applications with services in the healthcare sector [4, 5]. Internet of Medical Things (IoMT) is the combination of IoT with the health sector that is now developing the medicinal domain [6]. From the huge-scale IoT applications, the dependability of big data analysis with cloud computing is recognized. Ma *et al.*, developed a back end structure that allows cognitive services to the medical domain [7].

Glaucoma is an optic neuropathy characteristic with progressive degeneration of retinal ganglion tissues [8]. Some sample Glaucoma and normal images are shown in Fig. 1. Various kinds of glaucoma are connected by different etiologies with pathogenic factors, but, each consists of alterations in design as well as the action of an optic nerve. Glaucoma is assumed to be the 2nd important reason for vision failure on most people between the age of 40 to 80. Worldwide, people by glaucoma are estimated at approximately 64.3 million in the year 2013 with would enhance up to 76.0 million in 2020, etc [9]. Because of the asymptotic condition of glaucoma, behind analysis are often later. According to the population analysis, it is noticeable that 10-50% of humans are conscious as it is further prompting

between other people. With analyzing as well as avoiding vision failure, it is monitored in several works globally. Current works signified which glaucoma monitoring is expensive with improved use of initial automatic classifiers with the qualified assessment. Standard care to glaucoma monitoring occupies a normal time interval of two to three years. Doubtful reports are submitted for an ophthalmologist with executing further testing with exam to outcome support of investigative. If glaucoma is fully confirmed, it contains briefed patient data, slit lamp study, and so on. It contains Optical Coherence Tomography (OCT), which has been generally utilized to allow the design of optic nerves to occur in glaucoma. The images of the color fundus are executed in a combination of image processing methods to identify with an evaluation of eye disease.

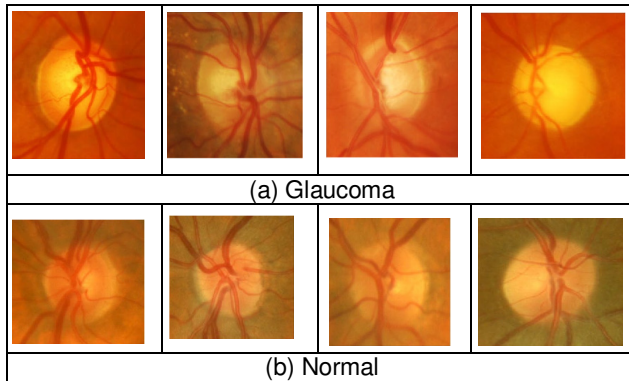


**Fig. 1.** Sample images (a) Glaucoma (b) Normal.

Accessibility of digital fundus cameras in initial care with larger applications in eye monitoring procedure explains the attention of monitoring glaucoma utilizing image modality. But individual analysis of fundus images utilized for recognition indications of glaucoma is a testing role that needs skill as well as experience. For resolving the difficulty, the important result gets in growing an automated identifying technique depending upon image processing models. A set of 4 major modifications takes place in the retinal design connected by glaucoma [10].

Several images processing system is planned for recognition of glaucoma. It focuses on localized with the segmentation of OD through huge glaucoma recognition concepts on primary feature extraction from images to increase little knowledge to trained several classifications. Extracted features recognize the connected information that occurs in images, linked by the capable for achieving the extensive demonstration related by clinical measurements. These recognition can be complete dependent on the probability of combining condensed features from pixel intensity values, Fourier Transform (FT) as well as B-splines coefficient, else utilize high order spectrum diagnosis with texture dependent features filtered from preprocessing images with Support Vector Machines (SVM) method, besides with feature extraction based on highest spectra with separate wavelet change through SVM classification, or executing empirical wavelet transform by lower squares SVM or with adaptive histogram equalized occupied by numerous filter banks method to generate local pattern processes which feed k-nearest neighbor (kNN)

classification. Earlier methods utilize the manner of identifying features in the image for training the classification connected by each identifying obtained from the image. At last, different manners grow diverse facts with the transfer of ONH to determine the designs that are exposable as well as identifying glaucoma.

The main contribution of this paper is the new automated glaucoma recognition and classifier approach for the identification of glaucoma diseases from the color fundus images. In the beginning, the real color fundus images hold a set of three RGB channels and the red channel gets extracted for further processes. Afterward, the contrast enhancement process gets executed by the use of an adaptive histogram equalization (AHE) model for improving the contrast level of the image. Subsequently, a bilateral filtering approach is given to discard the noise that exists in the image. Then, the Directional local ternary quantized extrema pattern (DLTerQEP) based feature extraction process takes place. Then, the extracted features undergo classification by the use of a Multi-Class Support Vector Machine (MSVM) model to classify the presence of glaucoma. The proposed model is tested using a DRISHTI-GS includes a sum of 101 retinal fundus images. The experimentation outcome presented the superiority of the projected model over the compared approaches.

## II. PROPOSED METHODS

The entire processes involved in the presented model are shown in Fig. 2. The figure indicated that different processes are present in the proposed model and the sub processes are explained below. To begin with, the real color fundus images holds a set of three RGB channels and the red channel gets extracted for further processes. Afterward, the contrast enhancement process gets executed by the use of the AHE model for improving the contrast level of the image. Subsequently, a bilateral filter can be employed for removing the noise that exists in the image. Then, DLTerQEP based feature extraction process is done. Then, the extracted features undergo classification by the use of the MSVM model to classify the presence of glaucoma.

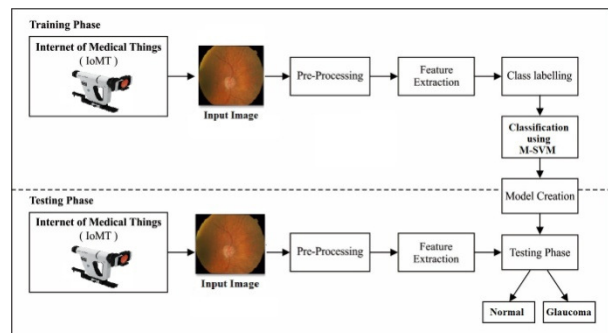


**Fig. 2.** Working flow of the presented model.

### A. Pre-processing

In this paper, the pre-processing occurs in 2 levels such as image improvement utilizing AHE with noise extraction utilizing BF. Initially, AHE concepts are used due to their benefits such as the efficiency with small

difficulties. It manages the image feature with the visual cause with increasing the share of grayscale values occurs in an image. It is essentially based on the possibility of shared operation. It resolving the complexities that occur in conventional methods with automatic identification through adjustable nature to the grayscale images. At the second level, BF is utilized on the images in grayscale type. Generally, some quantities of noise occurred in the image creation that may outcomes in the false recognition of cancer nodules. Therefore, it is required for effective identification of the noise preceding for a classifier. The view of BF based on the chosen weighting mechanism to average nearby pixels to eliminating the noises. In general method for represent BF contains a distance depend field filter part(  $k, k'$ ), with gray-value based on series filter part  $r( (fk), (fk'))$ :

$$\tilde{f}(k) = \frac{1}{N(x)} \int_{-\infty}^{\infty} f(k') d(k, k') r(f(k), f(k')) dk' \quad (1)$$

where  $i$  denotes the position of the center pixel,  $i'$  signifies the position of nearby pixels, and  $N(i)$  a normalized factor. If the field filters consist of the local average of nearby pixels, the series filter element forces the value dependent part for removing the filtering among edges. In order to field with series filter areas, usually, Gaussian functions are utilized with dependent on Euclidean pixel distance as provided under.

$$d(k, k') \propto \exp\left(-\frac{(k - k')^2}{2\sigma_d^2}\right) \quad (2)$$

$$r(f(x), f(x')) \propto \exp\left(-\frac{(f(x) - f(x'))^2}{2\sigma_f^2}\right) \quad (3)$$

with  $\sigma_d$  is a width attribute the size of kernel filter with  $\sigma_f$  the noise standard deviation of the supposed recreation value (e.g. attenuation noise standard deviation  $\sigma_a$ ). The contrast enhanced bilateral filtering image is displayed in Fig. 3.

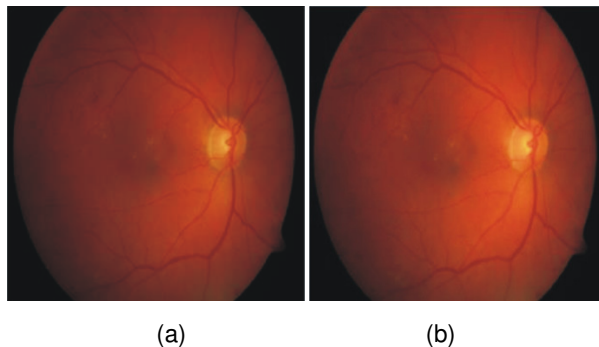


**Fig. 3.** (a) Input Image (b) Preprocesses Image.

### B. DLTerQEP based feature extraction

The models of the local structure are utilized to essential the DLTerQEP. It describes the spatial creation of local textures occur the ternary structure using local extrema with directional geometric formations [11]. Given the image in DLTerQEP, the local extrema in each direction are collected with the purpose of local difference between the middle pixels with its adjacent pixel utilizing the index of the models through pixel positions. The indexing of pixels occurs with write the group of 4 directional greater function computations. The Local

Directional Extrema Value (LDEV) to local model nearby image ( $I$ ) is resolved with

$$LDEV(q, r) = \sum_{q=1}^{k_1} \sum_{r=1}^{k_1} [I(q, r) - T(1 + \text{floor}\left(\frac{k_1}{2}\right), 1 + \text{floor}\left(\frac{k_1}{2}\right))] \quad (4)$$

where  $k_1 \times k_1$  denotes size of image. The group of 4 directional ternary extrema coding (DTEC) is collected based on the group of four directions such as 0, 45, 90 and 135 below diverse thresholds with utilize of local ternary pattern (LTP) models.

The DTEC coding is changed to pair of binary codes. Practically, the DLTerQEP enables to concatenate 4 directional extrema in every binary pattern of LTP. Through the multiplication of the binomial weights for every DTEC and LTP coding, the limited DLTerQEP values to a specific model ( $7 \times 7$ ) to describe the spatial association of the local models are signified as

$$DLTerQEP_{\alpha, P} = \sum_{w=0}^{P-1} DTEC_{(Lower)}^{(Upper)}, w 2^w \quad (5)$$

In total image, each DTECLTP (upper and lower) map lies in the series of 0 to 4095 (0 to  $2^P - 1$ ), then, the whole DTEC-LTP maps are created by the value lies in series of 0 to 8191 (0 to  $((2^P)^2) - 1$ ). The DLTerQEP is different from famous LBP method. It would filter spatial connection between the group of nearby occur in the local region beside the existing directions, but the LBP filters the connection in-between with nearby pixels. It removes the directional boundary features depending upon the local extrema that differs from available LBP. So, DLTerQEP capture detailed spatial data over LBP. The features extracted by this model are explained below.

**Color:** In order to denote the color attribute, the HSV color technique has been applied which is reliable from the human point of view. Hue is employed to identify the color difference as well as to determine the green or red color of light. Also, the Saturation concept denotes the intensity of white light which may be added in actual color. Generally, red is considered to be a more saturated color and pink is less saturated. The saturation could be computed by the amount of possible intensity of light. Therefore, the quantization of color is helpful in reducing computing difficulty. Additionally, it provides an efficient outcome and eliminates infinite units of color that could be termed as noise. Furthermore, HVS is assumed to be highly sensitive than hue model which must undergo the quantization process.

To present local color histogram, an image should be segmented to a similar size of  $3 \times 3$ , tetra-dimensional parts as well as extracts HSV which is combined with histogram should be quantized to 162 bins for all parts. Although it is composed of local color information, the final outcome obtained could not be used sufficiently. Color Histogram is mainly employed to obtain the gray color attributes from the given image. This model attempts to describe the image in the different factor of indicating the distribution of color bins which exists in the image. It counts the number of similar pixels and stores in a secured location. In order to extract a compact illustration, all histogram features have been

filtered that is with maximum peak value. Assuming that hue  $h$ , saturation  $s$ , value  $v$  are connected to the bin as dominant features of the rectangular segment that is generalized from the similar radius of  $[0, 1]$ . Hence, each image has a collection of 27-sided color vectors.

**Texture:** The texture is a significant parameter in such a way that major images hold it. As same to color features, the texture is been obtained from the local image area. Here, the co-occurrence matrix is said to be a 2-D histogram which computes the static of pairwise gray levels. The  $(i, j)$ th unit of co-occurrence matrix represents the measured likelihood as gray level  $i$  that is carried out along with gray level  $j$  from a specific displacement  $d$  as well as angle  $\theta$ . By the value selection of  $d$  and  $\theta$ , a single co-occurrence matrix could be accomplished. Most of the co-occurrence matrix is comprised of some texture features which are extracted. Consequently, each image is composed of a total of  $3 \times 3 (= 9)$  dimensional texture vectors.

### C. Classification

MSVM applies a multi-class function as defined in [12], also undergoes optimization along with a technique which is rapid in linear case. The training set  $(l_1, m_1) \dots (l_n, m_n)$  including labels  $m_p$  in  $[1, z]$ , it identifies the final outcome for following optimization issue while the period of training.

$$\begin{aligned} & \min 1/2 \sum_{p=1..z} w_p^* w_p + C/n \sum_{p=1..n} \xi_p \\ & \text{s.t. for all } m \text{ in } [1..z]: [ l_1 \cdot w_{mp} ] \geq [ l_1 \cdot w_m ] + 100 \cdot \Delta(m_1, m) - \xi_1 \\ & \text{for all } m \text{ in } [1..z]: [ l_n \cdot w_{mn} ] \geq [ l_n \cdot w_m ] + 100 \cdot \Delta(m_n, m) - \xi_n \end{aligned} \quad (6)$$

$C$  denotes the general regularizing attribute which trades off margin size as well as training error.  $\Delta(m_n, m)$  represent the loss function which is 0 if  $m_n$  is  $y$  and 1 otherwise.

For solving this optimization issue, MSVM employs a technique which is varied from other one in [1]. The applied model is based on Structural SVMs [2] and it is assumed to be SSVM. In case of linear kernels, MSVM V2.20 is rapid and runtime scales are linear with amount of training samples, whereas Non-linear kernels does not support at any cost. However, it is used as simple tutorial to learn the basic application of SSVM programming interface. Therefore, several details of SSVM could be obtained from this point.

## III. PERFORMANCE VALIDATION

### A. Dataset

The proposed technique undergoes testing against the DRISHTI-GS dataset, that contains around 101 retinal fundus images for segmenting and classifying the OD area [13]. Initially, doctors find the people affected by Glaucoma with the help of practical examinations. The images are obtained from patients at the age of 45-85 years. Table 1 contains the data which is relevant to a given dataset. The predefined 101 images present in the dataset and group of 31 images come with respect to ordinary class and collection of 70 images belongs to Glaucoma class.

The process of selecting red channels from the simulation result of filtered image denotes the contrast feature between OD region as well as background is shown in Fig. 4.

**Table 1: Dataset Description.**

Description	Value
Total Number of Images	101
Normal images	31
Glaucoma images	70
Sample Data collected [13]	

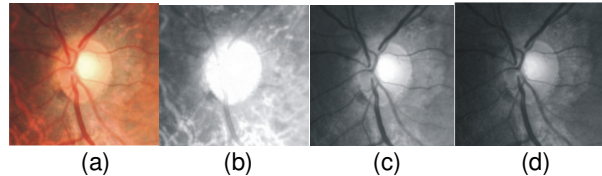


**Fig. 4.** Extracted output (a) Input image. (b) R channel. (c) G channel. (d) B channel.

Alternatively, the median filter has been applied to the red channel to eliminate the noise in image which leads to forming a maximum visible OD area. Additionally, it reduces the clarity of blood vessels in the OD portion. Here, threshold values could be achieved from the Otsu technique that is influenced when isolating the OD part from the background and alternate images. Thus, divided threshold images are computed under the application of opening notation to attain an efficient segmenting of the OD area that tends to produce a binary image. Therefore, the segmented image which has been originated would be verified with the help of an image in order to obtain maximum accuracy in the classification process. Furthermore, contrast is often used for determining the varying brightness among all images. As shown in Fig. 5, red channels offer a high contrast rate of 11.155 which signifies that brightness has been varied to the maximum value when compared with other methods. But, green and blue channels resulted in only less contrast values of 2.708 and 0.439 respectively. Simultaneously, the OD objects, as well as background, could be classified under the red channel.

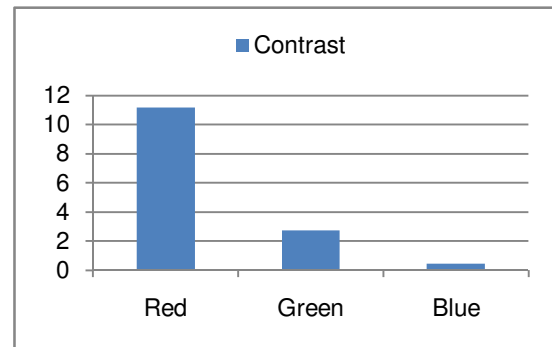


**Fig. 5.** Average texture features under contrast.

The optimal outcome of employed techniques have been compared and a brief examination has been performed using available methods from similar datasets. Hence, the derived and compared values are provided in Table 2 and Figs. 6-8.

On validating the results with respect to sensitivity, it is apparent that the RF, SVM, KNN, and NB offers poor and identical outcome with the same sensitivity value of 50. However, the presented model offered a maximum sensitivity value of 81.86.

**Table 2: Comparative analysis of different models.**

Model	Sensitivity	Specificity	Accuracy
DLTerQEP+MSVM	81.86	92.85	87.43
RF	50	0	80.00
SVM	50	0	70.20
KNN	50	50	52.50
NB	50	50	61.20

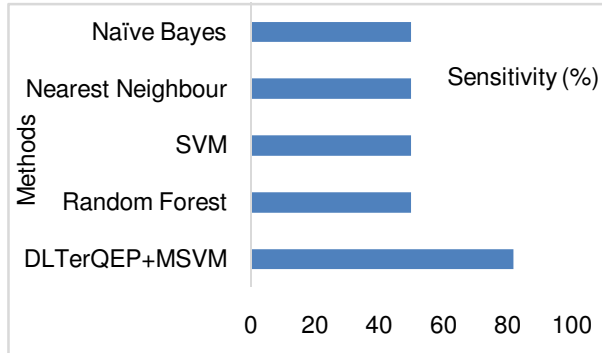


**Fig. 6.** Sensitivity analysis of different methods.

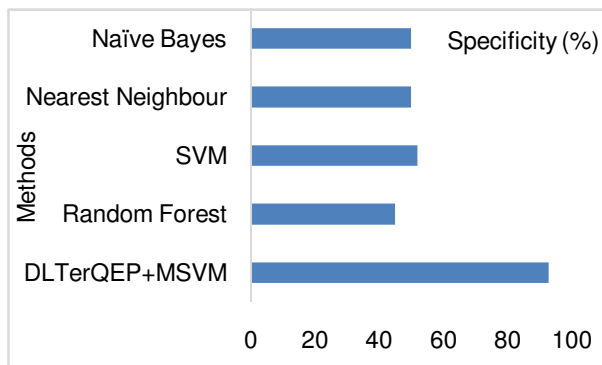


**Fig. 7.** Specificity analysis of different methods.

Likewise, on validating the results with respect to specificity, it is apparent that the RF, SVM shows the worst classification by attaining the least value of 0 specificity. In addition, KNN and NB offer poor and identical outcomes with the same specificity value of 50. However, the presented model offered a maximum sensitivity value of 92.85.

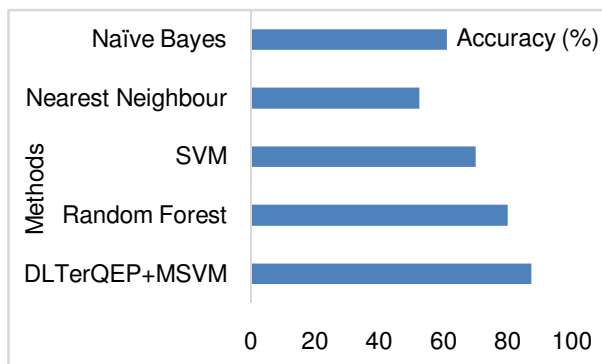


**Fig. 8.** Accuracy analysis of different methods.

Similarly, on the validation of the performance with respect to the accuracy, it is evident that the KN and NB models show the worst classification by attaining the least accuracy values of 52.50 and 61.20 respectively. In addition, RF and SVM offer poor outcomes with the minimum accuracy values of 80 and 70.20 respectively. However, the presented model offered maximum classification with the highest accuracy value of 87.43. These values verified the enhanced classifier results of the presented approach over the existing approaches.

#### IV. CONCLUSION

This paper has introduced an IoT and Cloud-based Glaucoma detection and classification model for color fundus images. The presented model involves dissimilar levels of preprocessing, feature extraction and classification. Upon the evaluation of the projected approach on the benchmark dataset, the superior outcome of the proposed model gets revealed. By comparing the results attained by the presented model over the compared methods, it is observed that the maximum classification performance is offered by the presented model with a sensitivity of 81.86, the specificity of 92.85 and accuracy of 87.43.

#### V. FUTURE SCOPE

In the future, the presented model can be implemented in a real-time environment to assist patients in remote areas.

**Conflict of Interest.** The authors don't have any conflicts of interest.

#### REFERENCES

- [1]. Ganesan, M., & Sivakumar, N. (2017). A Survey on IoT Related Patterns. *International Journal of Pure and Applied Mathematics*, 117(19), 365-369.
- [2]. Ganesan, M., Devi, K. S., Vasantharaj, S., Ruth, A. B., Prithi, N., & Kumar, K. P. (2015). Preservation of Implanted Medical Device's Battery Power. In *Proceedings of the 2015 International Conference on Advanced Research in Computer Science Engineering & Technology (ICARCSET)*, 61-70.
- [3]. An, G., Omodaka, K., Hashimoto, K., Tsuda, S., Shiga, Y., Takada, N., & Nakazawa, T. (2019). Glaucoma diagnosis with machine learning based on optical coherence tomography and color fundus images. *Journal of Healthcare engineering*, 1-9.
- [4]. Paul, P., Dutta, N., Biswas, B. A., Das, M., Biswas, S., Khalid, Z., & Saha, H. N. (2018). An Internet of Things (IoT) Based System to Analyze Real-time Collapsing Probability of Structures. In *2018 IEEE 9th Annual Information Technology, Electronics and Mobile Communication Conference (IEMCON)*. 1070-1075.
- [5]. Ganesan, M., Kumar, A. P., Krishnan, S. K., Lalitha, E., Manjula, B., & Amudhavel, J. (2015). A novel based algorithm for the prediction of abnormal heart rate using Bayesian algorithm in the wireless sensor network. In *Proceedings of the 2015 International Conference on Advanced Research in Computer Science Engineering & Technology (ICARCSET)*.pp. 53-62.
- [6]. Maitra, M., & Chatterjee, A. (2006). A Slantlet transform based intelligent system for magnetic resonance brain image classification. *Biomedical Signal Processing and Control*, 1(4), 299-306.

- [7]. Ma, Y., Wang, Y., Yang, J., Miao, Y., & Li, W. (2017). Big health application system based on health internet of things and big data. *IEEE Access*, 5, 7885-7897.
- [8]. Weinreb, R. N., Aung, T., & Medeiros, F. A. (2014). The pathophysiology and treatment of glaucoma: a review. *Jama*, 311(18), 1901-1911.
- [9]. Tham, Y. C., Li, X., Wong, T. Y., Quigley, H. A., Aung, T., & Cheng, C. Y. (2014). Global prevalence of glaucoma and projections of glaucoma burden through 2040: a systematic review and meta-analysis. *Ophthalmology*, 121(11), 2081-2090.
- [10]. Haleem, M. S., Han, L., Van Hemert, J., & Li, B. (2013). Automatic extraction of retinal features from colour retinal images for glaucoma diagnosis: a review. *Computerized medical imaging and graphics*, 37(7-8), 581-596.
- [11]. Deep, G., Kaur, L., & Gupta, S. (2016). Directional local ternary quantized extrema pattern: a new descriptor for biomedical image indexing and retrieval. *Engineering science and technology, an international journal*, 19(4), 1895-1909.
- [12]. Lin, W. M., Wu, C. H., Lin, C. H., & Cheng, F. S. (2008). Detection and classification of multiple power-quality disturbances with wavelet multiclass SVM. *IEEE transactions on power delivery*, 23(4), 2575-2582.
- [13]. <http://cvit.iiit.ac.in/projects/mip/drishti-gs/mip-dataset2/Home.php>

**How to cite this article:** Anandh, R. and Indirani, G. (2020). IoT and Cloud based Feature Extraction and Classification Model for Automatic Glaucoma Detection. *International Journal on Emerging Technologies*, 11(2): 13-18.